Typicalness-Aware Learning for Failure Detection

Yijun Liu[1] **Jiequan Cui**[2] **Zhuotao Tian**[1✉] **Senqiao Yang**[3]
Qingdong He[4] **Xiaoling Wang**[1] **Jingyong Su**[1✉]
{liuyijun}@stu.hit.edu.cn
[1]Harbin Institute of Technology (Shenzhen) [2]Nanyang Technological University
[3]The Chinese University of Hong Kong [4]Tencent Youtu Lab

Abstract

Deep neural networks (DNNs) often suffer from the overconfidence issue, where incorrect predictions are made with high confidence scores, hindering the applications in critical systems. In this paper, we propose a novel approach called Typicalness-Aware Learning (TAL) to address this issue and improve failure detection performance. We observe that, with the cross-entropy loss, model predictions are optimized to align with the corresponding labels via increasing logit magnitude or refining logit direction. However, regarding atypical samples, the image content and their labels may exhibit disparities. This discrepancy can lead to overfitting on atypical samples, ultimately resulting in the overconfidence issue that we aim to address. To tackle the problem, we have devised a metric that quantifies the typicalness of each sample, enabling the dynamic adjustment of the logit magnitude during the training process. By allowing atypical samples to be adequately fitted while preserving reliable logit direction, the problem of overconfidence can be mitigated. TAL has been extensively evaluated on benchmark datasets, and the results demonstrate its superiority over existing failure detection methods. Specifically, TAL achieves a more than 5% improvement on CIFAR100 in terms of the Area Under the Risk-Coverage Curve (AURC) compared to the state-of-the-art. Code is available at https://github.com/liuyijungoon/TAL.

1 Introduction

Failure detection plays a vital role in machine learning applications, particularly in high-risk domains where the reliability and trustworthiness of predictions are crucial. Applications such as medical diagnosis [8], autonomous driving [18, 41, 42], and other visual perception tasks [21, 37, 31, 24, 34, 29, 36, 28, 35] require accurate assessments of prediction confidence before making critical decisions. The goal of failure detection is to enhance the reliability and trustworthiness of predictions, ensuring that high-confidence predictions are relied upon while low-confidence predictions are appropriately rejected [25, 46]. This is essential for maintaining the safety and effectiveness of these applications.

Indeed, deep neural networks (DNNs) trained using the cross-entropy loss often suffer from the issue of overconfidence. This leads to unreliable confidence scores, which in turn hinder the effectiveness of failure detection methods. It is common for models to make incorrect predictions with high confidence scores, sometimes even close to 1.0. A recent study called LogitNorm [39] has shed light on this problem. It reveals that the softmax cross-entropy loss can cause the magnitude of the logit vector to continue increasing, even when most training examples are correctly classified. This phenomenon contributes to the model's overconfidence.

To alleviate the overconfidence problem, LogitNorm [39] proposes assigning a constant magnitude to decouple the influence of the magnitude during optimization. The cross-entropy loss with the

✉: Corresponding Authors. Email: tianzhuotao@hit.edu.cn, sujingyong@hit.edu.cn

38th Conference on Neural Information Processing Systems (NeurIPS 2024).

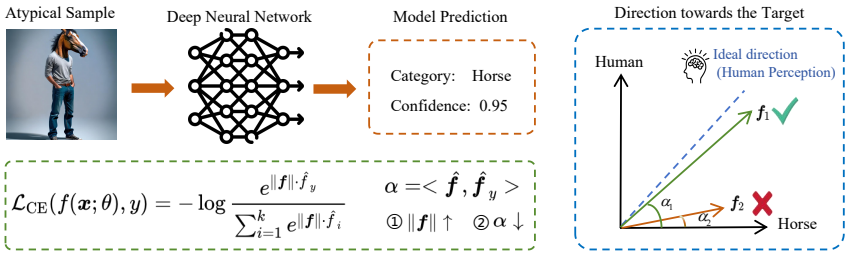

Figure 1: Illustration of the motivation. We observe that directly aligning the predictions of atypical samples to the target label is not appropriate, causing overconfidence (horse with 95% confidence). Instead, the confidence should be aligned with the human perception. During training, the cross-entropy loss increases the magnitude $\|\boldsymbol{f}\|$ and adjusts their direction towards the target (represented by the angle α). Consider this example where an image of a human body with a horse head is presented, the loss may optimize towards $\boldsymbol{f}_2$ in the blue box, which is not the ideal outcome direction. Instead, it would be better to optimize towards $\boldsymbol{f}_1$, rather than being biased towards either one, ensuring a more balanced and unbiased representation and allowing for a more accurate estimation of confidence.

decoupled logit vector $\boldsymbol{f} = f(\boldsymbol{x};\Theta)$ is defined as what follows:

$$\mathcal{L}_{\text{CE}}(\boldsymbol{f},y) = -\log \frac{e^{\|\boldsymbol{f}\|\cdot\hat{\boldsymbol{f}}_y}}{\sum_{i=1}^{C} e^{||f||\cdot\hat{\boldsymbol{f}}_i}}, \tag{1}$$

where Θ is the parameters of the DNN model, $\boldsymbol{x}$ is the input image with label y, the logit vector $\boldsymbol{f}$ is decoupled into the *magnitude* $\|\boldsymbol{f}\|$ and the *directions* $\hat{\boldsymbol{f}}$. Based on the decomposition of the logit vector in Eq. (1), we can observe that the overconfidence issue could stem from either increasing $\|\boldsymbol{f}\|$ or decreasing α (the angle between the directions of prediction and label) during training.

Key observation & Motivation. Following the exclusion of the logit magnitude's impact by LogitNorm [39], we posit that the risk of the overconfidence issue still arises from logit directions. Typical samples, which have clear contextual information, help models generalize well. However, optimizing the direction for ambiguous atypical samples can still cause overconfidence. In these cases, the labels do not match the image context well. Aligning the logit direction of atypical samples may still lead to high softmax scores near 1.0 which worsens the overconfidence problem.

According to previous work [50, 43], the definitions of typical and atypical samples are based on their semantic similarity to most samples and the ease with which the model learns them. Specifically:

- *Typical samples* are those that exhibit similarity to a majority of other samples at the semantic level. These samples possess typical features that are easier for deep neural networks to learn and generalize.
- *Atypical samples*, on the other hand, differ significantly from other samples at the semantic level. They pose a challenge for the model to generalize due to their uniqueness. These samples are often located near the decision boundary, causing the model to have higher uncertainty in making predictions for them.

In Fig. 1, we present an atypical example to illustrate the issue at hand. Despite the ground-truth label being a horse, the image depicts a horse with a human body, which could reasonably be predicted as either a human or a horse with a confidence score of around 50%. However, the model incorrectly predicts the image as a horse with an excessively high confidence score of 95%. Upon examining Eq. (1), we observe that the confidence score is determined by two crucial factors: magnitude and direction. This prompts an important question regarding the decoupling of these factors to determine which one is more reliable in accurately approximating real confidence. Addressing this inquiry is essential for effective failure detection.

Our approach. Based on the aforementioned observations, we propose a novel approach called *Typicalness-Aware Learning (TAL)*. TAL dynamically adjusts the magnitudes of logits based on the typicalness of the samples, allowing for differentiated treatments of typical and atypical samples. By doing so, TAL aims to mitigate the adverse effects caused by atypical samples and emphasizes that the direction of logits serves as a more reliable indicator of model confidence. In the blue dashed box of Fig. 1, we provide an example that illustrates the impact of TAL on an atypical sample. The logit vector could be changed from $\boldsymbol{f}_2$ to $\boldsymbol{f}_1$, indicating that the scores obtained with $\hat{\boldsymbol{f}}$ for both "horse"

and "human" become nearly equal. This alignment better aligns with human perception, highlighting the effectiveness of TAL in improving model confidence estimation.

The proposed TAL approach is model-agnostic, making it easily applicable to models with various architectures, such as CNN [12] and ViT [6]. Experimental results on benchmark datasets, including CIFAR10, CIFAR100, and ImageNet, demonstrate the superiority of TAL over existing failure detection methods. Specifically, on CIFAR100, our method achieves a significant improvement of more than 5% in terms of the Area Under the Risk-Coverage Curve (AURC) compared to the state-of-the-art method [48].

In summary, the main contributions of this paper are as follows:

- We propose a new insight that the overconfidence might stem from the presence of atypical samples, whose labels fail to accurately describe the images. This forces the models to conform to these imperfect labels during training, resulting in unreliable confidence scores.
- In order to mitigate the issue of overfitting on atypical samples, we introduce the Typicalness-Aware Learning (TAL), which enables the identification and separate optimization of typical and atypical samples, thereby alleviating the problem of overconfidence.
- Extensive experiments demonstrate the effectiveness and robustness of TAL. Besides, TAL has no structural constraints to the target model and is complementary to other existing failure detection methods.

2 Background and Preliminary

Prior to introducing our method, we present the background of Failure Detection (FD). Additionally, we highlight the distinctions between failure detection and two closely related concepts: Confidence Calibration (CC) and Out-of-Distribution detection (OoD-D).

Failure Detection. Failure detection (FD) [17, 25, 48, 49] aims to differentiate between correct and incorrect predictions by utilizing the ranking of their confidence levels. In particular, a confidence-rate function $\kappa(\cdot)$ is employed to assess the confidence level of each prediction. High-confidence predictions are accepted, while low-confidence predictions are rejected. By using a predetermined threshold $\delta \in \mathbb{R}^+$, users can make informed decisions based on the following function g:

$$g(\boldsymbol{x}) = \begin{cases} \text{accept} & \text{if } \kappa(\boldsymbol{x}) \geq \delta, \\ \text{reject} & \text{otherwise.} \end{cases} \tag{2}$$

where $\kappa(\cdot)$ denotes a confidence-rate function, such as the maximum softmax probability.

Failure Detection vs. Confidence Calibration. Confidence calibration (CC) [32, 22, 26, 44] primarily emphasizes the alignment of predicted probabilities with the actual likelihood of correctness, rather than explicitly detecting failed predictions as in FD. The goal of CC is to ensure that the predictive confidence is indicative of the true probability of correctness:

$$P\left(\hat{y} = y \mid \hat{p} = p^*\right) = p^*, \forall p^* \in [0, 1]. \tag{3}$$

This implies that when a model predicts a set of inputs x to belong to class y with a probability p^*, we would expect approximately p^* of those inputs to truly belong to class y.

However, as observed by [48], models calibrated with CC algorithms do not perform well in FD. Traditional metrics used to evaluate CC, such as the Expected Calibration Error (ECE [27]), do not accurately reflect performance in FD scenarios. Instead, alternative metrics like the Area Under the Risk-Coverage Curve (AURC [7]) and the Area Under the Receiver Operating Characteristic Curve (AUROC [2]) are recommended for assessing FD performance.

Failure Detection vs. Out-of-Distribution Detection. While both Out-of-Distribution Detection (OoD-D) and failure detection tasks aim to enhance confidence reliability, they have distinct objectives, as depicted in Fig. 2. OoD-D focuses on rejecting predictions of semantic shift while accepting in-distribution predictions. However, it does not explicitly address the rejection of cases affected by covariate shifts. Additionally, through empirical observations in Sec. 4, we find that OoD-D methods are not well-suited for the Failure Detection task.

Traditional Failure Detection (Old FD) vs. New Failure Detection (New FD). Traditional failure detection methods [48, 49, 25] primarily focus on assessing the accuracy of predictions for in-distribution data. They also evaluate the discriminative performance of distinguishing correct and

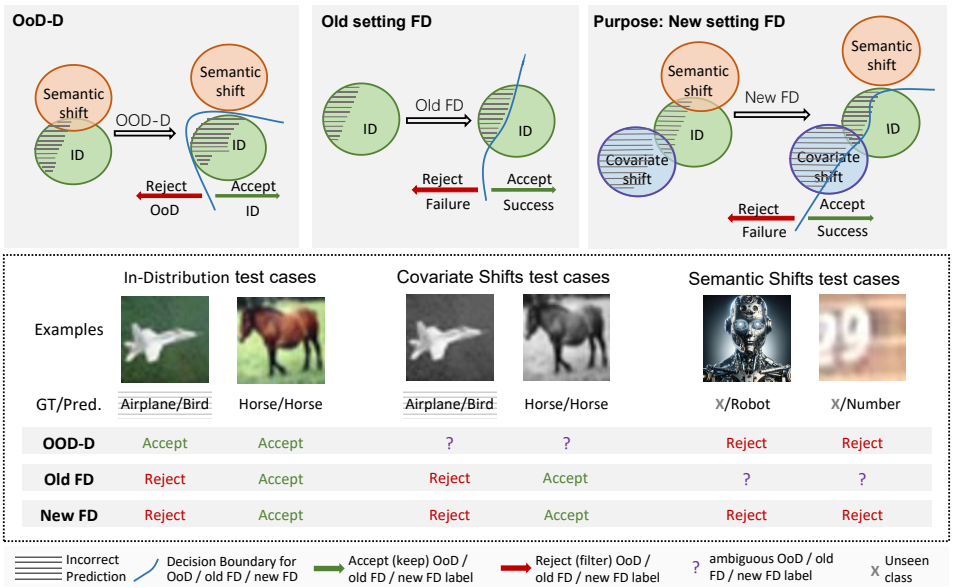

Figure 2: The differences between closely related tasks. The blue curve represents the decision boundary, and the shaded area in the figure indicates incorrect predictions. (a) illustrates the objective of OoD-D tasks to reject predictions with semantic shifts and accept in-distribution predictions, without concern for predictions with covariate shifts. (b) shows the old setting of FD tasks, accepting correct in-distribution predictions and rejecting incorrect out-of-distribution predictions. (c) displays the new setting of FD tasks, accepting correct in-distribution predictions and correct predictions with covariate shifts, while rejecting incorrect in-distribution predictions, incorrect predictions with covariate shifts, and predictions with semantic shifts. (d) illustrates examples of OoD-D, Old FD, and New FD tasks. A classifier trained on CIFAR10 [20] is evaluated on 6 images under a whole range of relevant distribution shifts: For instance, the 3rd and the 4th images in grayscale depict an airplane and a horse which encounter covariate shifts from that in the original CIFAR10. The 5th and the 6th images depict samples belonging to unseen categories with semantic shifts.

incorrect predictions for covariate shift data based on confidence scores. While these approaches address certain aspects of distribution shifts, they overlook the semantic shifts.

To address the limitations of Out-of-Distribution Detection (OoD-D) and traditional failure detection (Old FD) methods, [17] proposes a new setting called New FD. The objective of New FD is to accept correct predictions for both in-distribution and covariate shift samples, while rejecting incorrect predictions for all possible failures, including in-distribution, covariate shift, and semantic shift samples. Compared to OoD-D and Old FD, it enables more effective decision-making in real world.

3 Method

In this section, we present our proposed strategy called Typicalness-Aware Learning (TAL), as shown in Fig. 3. First, in Sec. 3.1, we address the shortcomings of existing training objectives and identify overfitting of atypical samples as a potential cause of overconfidence. Next, in Sec. 3.2, we outline the methodology used to calculate the "typicalness" of samples, enabling selective optimization and mitigating the negative impact of atypical samples. Finally, in Sec. 3.3, we introduce the TAL strategy, which incorporates the computed typicalness values for individual samples, resulting in improved performance for the failure detection task.

3.1 Revisit the Cross-entropy Loss

In Eq. (1), the optimization of the cross-entropy loss involves either increasing the magnitude of the logits or aligning them better with the labels. However, LogitNorm [39] researchers have observed that as the training progresses and the model becomes more accurate in classifying samples, it tends to generate significantly larger logit magnitudes, leading to overconfidence. To address this issue,

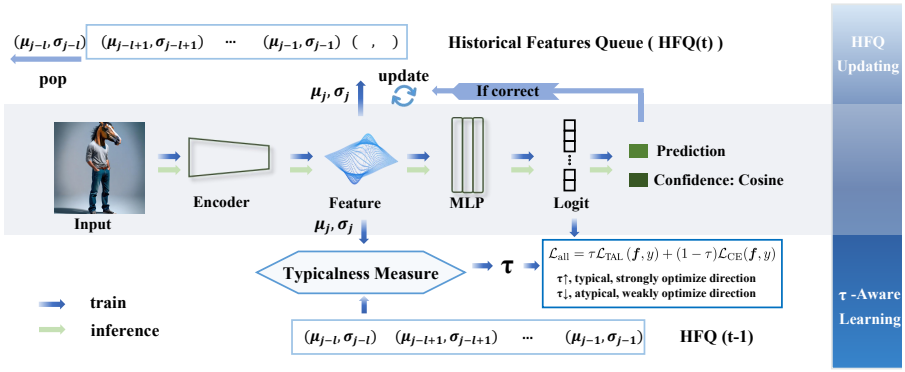

Figure 3: The framework of TAL. During training, statistical information (mean μ_j and variance σ_j) of features from correct predictions updates the Historical Features Queue (HFQ) at time-step t. The typicalness measure τ is calculated by comparing these statistics between the current batch and the HFQ. This τ influences the overall loss calculation, guiding the model to differentiate between atypical and typical samples. In the inference phase, TAL operates similarly to a model trained with conventional cross-entropy. Confidence is derived from the cosine similarity of the predicted logit direction, emphasizing our approach of using direction as a more reliable confidence metric. The framework distinguishes between typical (high τ) and atypical (low τ) samples, influencing the optimization process accordingly.

LogitNorm introduces a constant magnitude T in Eq. (4) to mitigate the problem:

$$\mathcal{L}_{\text{logit\_norm}}(\boldsymbol{f}, y) = -\log \frac{e^{\hat{\boldsymbol{f}}_y * \mathrm{T}}}{\sum_{i=1}^{k} e^{\hat{\boldsymbol{f}}_i * \mathrm{T}}}. \tag{4}$$

By keeping the magnitude constant in Eq. (4), the model places greater emphasis on producing features that align more closely with the target label in terms of direction, in order to minimize the training loss. However, as shown in Fig. 1, the presence of atypical samples with ambiguous content and labels may still cause overconfidence. Hence, it is imperative to devise a method that allows for the differentiation and separate optimization of typical and atypical samples.

Drawing inspiration from the cognitive process of human decision-making, it is reasonable to distinguish between typical and atypical samples by leveraging the knowledge acquired during the training phase. This approach allows us to effectively mitigate the negative effects of atypical samples, thereby preventing the occurrence of erroneous overconfidence.

3.2 Distinguish Typical and Atypical Samples

To differentiate typical samples from atypical ones, we introduce a method for evaluating typicalness and implement typicalness-aware learning (TAL). This approach entails calculating the mean and variance of the feature representations. Specifically, we calculate the mean and variance of each sample's feature channels based on insights from CORES [30]. The insight stems from the observation that in-distribution samples show larger magnitudes (mean) and variations (variance) in convolutional responses across channels compared to OoD samples, which are a type of atypical sample. The mean response of OOD samples is smaller than correct ID samples, as shown in Fig. 5(a). These statistical characteristics are subsequently compared to a set of historical data, representing typical samples, stored in a structured queue known as the "Historical Feature Queue" (HFQ). By comparing the statistical features of the input samples to those in the HFQ, we can quantify their typicalness.

Initialize and update HFQ. We commence the process by initializing the HFQ, denoted as Q, with a predetermined size equivalent to the number of samples in the training dataset. This structured queue is responsible for retaining the mean and variance of feature representations for typical samples identified throughout the training phase.

To establish the initial state of the queue, we do not adopt the model trained from scratch. Instead, we employ a model that has been trained for a few epochs, corresponding to a small portion (λ) of the total training epochs. This approach ensures the quality of the queue during the early stages of training. In this study, we set $\lambda = 0.05$, which corresponds to 5% of the total training duration.

During this initialization phase, for each batch of data, we calculate the mean (μ) and variance (σ^2) of the feature vectors for each correctly predicted sample. Each sample in the queue stores its statistical features, denoted as follows, given a prediction $\hat{y}$ and the ground truth label y:

$$Q = \{(\mu_i, \sigma_i^2) \mid \hat{y}_i = y\} \tag{5}$$

where μ_i and σ_i^2 represent the mean and variance of the feature vectors of the i-th sample, respectively.

Once initialized, the statistics (mean and variance) of accurately predicted samples in each batch are directly added to the queue, as shown in Fig. 3. The queue has a fixed length of 20,000, and the ablation study is provided in Sec 4.3. The queue is updated using a First-In-First-Out (FIFO) approach, guaranteeing that it preserves a representative assortment of typical samples observed throughout the training process, while also adapting to the evolving data distributions. We empirically find this simple strategy works well in our experiments.

Typicalness assessment. To evaluate the typicalness τ of a new sample, we first calculate the mean (μ_{new}) and variance (σ^2_{new}) of its features $\boldsymbol{f}$. Subsequently, we compute the $L2$ distance d between the feature distribution of the new sample, represented by μ_{new} and σ^2_{new}, and the distributions of the features stored in the HFQ, denoted as $(\mu_j, \sigma_j^2) \in Q$. Finally, we normalize the resulting distance using min-max normalization to obtain the typicalness τ.

$$d = \min_{(\mu_j, \sigma_j^2) \in Q} W((\mu_{new}, \sigma^2_{new}), (\mu_j, \sigma_j^2)), \tag{6}$$

$$\tau = 1 - \frac{d - d_{min}}{d_{max} - d_{min}}. \tag{7}$$

Where d_{min} and d_{max} represent the minimum and maximum distances of samples in the batch. Eq. (7) normalizes the value of τ within the range of $[0, 1]$, then τ can serve as a indicator of sample typicalness. A high τ value suggests that the sample is highly typical compared to the historical data. Conversely, a low τ value indicates an atypical or anomalous sample.

3.3 Typicalness-Aware Learning

Sec. 3.1 highlights the potential negative impact of atypical samples on the training process. Building upon the insights provided in Sec. 3.2, we now introduce Typicalness-Aware Learning (TAL) in this section. TAL leverages the typicalness τ to distinguish between typical and atypical samples during the optimization process. This approach aims to mitigate the issue of overconfidence that arises from the presence of atypical samples.

The training objective of TAL. The training objective of TAL is defined by incorporating an additional loss term $\mathcal{L}_{\text{TAL}}$. This is achieved by modifying the LogitNorm equation, denoted as Eq. (4), to Eq. (8) where the samples $\boldsymbol{x}$ are assigned with dynamic magnitudes $T(\tau)$ based on typicalness τ.

$$\mathcal{L}_{\text{TAL}}(\boldsymbol{f}, y) = -\log \frac{e^{\hat{\boldsymbol{f}}_{\boldsymbol{y}} * T(\tau)}}{\sum_{i=1}^{k} e^{\hat{\boldsymbol{f}}_i * T(\tau)}}. \tag{8}$$

Dynamic magnitude $T(\tau)$. Given the upper bound T_{max} and the lower bound T_{min}, the dynamic magnitude $T(\tau)$ can be obtained via:

$$T(\tau) = T_{\text{min}} + (1 - \tau) \times (T_{\text{max}} - T_{\text{min}}), \tag{9}$$

where we empirically set T_{max} and T_{min} to 10 and 100, and they perform well on different benchmarks. The ablation study on different values is shown in Sec. 4.3.

Specifically, in Eq. (9), a *smaller* magnitude $T(\tau)$ will be assigned to *typical* samples with large τ, and a *larger* magnitude $T(\tau)$ will be assigned to *less typical* samples with smaller τ, enabling different treatments for typical/atypical samples. In this manner, for atypical samples, a higher value of $T(\tau)$ reduces the influence that pulls them towards the label direction. This helps prevent their logit directions from being excessively optimized.

In other words, the inverse proportionality between $T(\tau)$ and τ encourages the model to yield directions of $\boldsymbol{f}$ that are well-aligned with the labels for the typical samples with large τ by assigning a small magnitude $T(\tau)$. Conversely, for atypical samples with small τ, the directions are not required

to be as precise as the typical ones as the current $T(\tau)$ is large, to mitigate the adverse impacts brought by the ambiguous label. To this end, *the direction $\hat{\boldsymbol{f}}$ can serve as a more reliable indicator of the model confidence*.

The overall optimization.

Fig. 3 illustrates the TAL framework, showing both training and inference processes. During the training process, we utilize both the proposed TAL loss $\mathcal{L}_{\text{TAL}}$ and cross-entropy loss $\mathcal{L}_{\text{CE}}$ as it exhibits stronger feature extraction capabilities than LogitNorm [39]. The overall loss is:

$$\mathcal{L}_{\text{all}} = \tau \mathcal{L}_{\text{TAL}}\left(\boldsymbol{f}, y\right) + (1-\tau)\mathcal{L}_{\text{CE}}(\boldsymbol{f}, y) \tag{10}$$

The TAL loss, denoted as $\mathcal{L}_{\text{TAL}}$, is utilized to optimize the directions of reliable typical samples with large typicalness τ, as well as potentially some atypical samples with small τ.

The CE loss (not only relying on the CE loss, as it is regulated by τ) for atypical samples enables the optimization of both direction and magnitude. This may help reduce the adverse effects of atypical samples on the direction, enhancing the reliability of direction as a confidence indicator. This ensures that the optimization force on the logit directions of atypical samples is weaker compared to that of typical samples. The inference process does not involve the calculation of typicalness, and the only difference from the normal inference process is that our method uses Cosine as the confidence score.

To summarize, our proposed approach, as indicated in Eq. (10), enables models to selectively and adaptively optimize typical and atypical samples according to their typicalness values. This strategy enhances the reliability of feature directions as indicators of model confidence, ultimately improving the performance on failure detection task.

4 Experiments

To evaluate the effectiveness of the proposed Typicalness-Aware Learning (TAL) strategy, we conduct extensive experiments on various datasets, network architectures, and failure detection (FD) settings. More details such as the training configuration can be found in Appendix A.

Datasets and models. We first evaluate on the small-scale CIFAR-100 [20] dataset with SVHN [11] as its out-of-distribution (OOD) test set. To demonstrate scalability, we further conduct experiments on large-scale ImageNet [5] using ResNet-50, with Textures [3] and WILDS [19] serving as OOD data. For CIFAR-100, we verify TAL's effectiveness across diverse architectures including ResNet [13], WRNet [45], DenseNet [15], and the transformer-based DeiT-Small [38]. Detailed experimental results are provided in Appendix C.

Three settings. We evaluate TAL under three different settings: Old FD setting, OOD detection setting, and New FD setting (detailed in Section 2). While Old FD distinguishes between correct and incorrect in-distribution predictions, and OOD detection identifies out-of-distribution samples, our New FD setting aims to separate correctly predicted in-distribution samples from both misclassified and out-of-distribution samples. We maintain a 1:1 ratio between in-distribution and out-of-distribution samples in testing, and also report results for Old FD and OOD detection settings for completeness.

Baselines. We compare our proposed TAL method against classical Maximum Softmax Probability (MSP), MaxLogit[14], Cosine[47], Energy [23], Entropy [33], Mahalanobis [4], Gradnorm [16], SIRC [40] and recent LogitNorm [39], OpenMix [49] and (FMFP) [48]. It is worth noting that FMFP focuses on improving accuracy for failure detection.

Evaluation metrics. To comprehensively assess the performance of TAL in failure detection, we adopt three widely recognized evaluation metrics [17, 48, 9], including Area Under the Risk-Coverage Curve (AURC), Area Under the Receiver Operating Characteristic Curve (AUROC), False Positive Rate at 95% True Positive Rate (FPR95).

4.1 Comparisions with the State-of-the-art on CIFAR

Evaluation with CNN-based architectures. As shown in Tab. 1, our TAL strategy outperforms existing methods in New FD settings. Here are the key observations: 1) OoD methods like Energy and LogitNorm do not achieve satisfactory performance in the FD task. Please refer to Appendix B

for explanation. 2) TAL consistently surpasses the baseline MSP and MaxLogit across various network architectures by a large margin. 3) In terms of comparison with FMFP, the prior SOTA method in the field of FD, our analysis reveals that TAL is complementary to the FMFP method and exhibits superior performance when combined with it. 4) Regarding Openmix, the metrics presented demonstrate that it falls short when compared to TAL.

Table 1: Evaluation results of the proposed TAL on CIFAR100.

Architecture	Method	Old setting FD			OOD Detection			New setting FD			ID-ACC
		AURC↓	FPR95↓	AUROC↑	AURC↓	FPR95↓	AUROC↑	AURC↓	FPR95↓	AUROC↑	
						CIFAR100 vs. SVHN					
ResNet110 [13]	MSP[14]	99.83	67.49	84.07	293.44	83.41	74.55	376.42	66.92	84.00	72.01
	Cosine [47]	96.53	65.15	84.42	271.13	78.30	79.31	361.87	56.23	86.93	72.01
	Energy [23]	135.85	74.66	77.20	275.39	83.18	77.78	387.44	66.96	83.21	72.01
	MaxLogit[14]	133.19	72.33	77.96	275.85	82.53	77.73	385.81	65.08	83.56	72.01
	Entropy [33]	100.05	66.28	84.12	287.62	81.20	75.93	373.49	61.33	84.73	72.01
	Mahalanobis [4]	114.21	73.48	80.41	263.49	72.70	80.55	368.55	58.74	85.74	72.01
	Gradnorm [16]	369.86	98.82	35.30	490.21	98.17	49.26	679.48	98.69	42.76	72.01
	SIRC [40]	100.56	66.37	84.01	287.93	81.03	75.90	374.12	61.29	84.65	72.01
	LogitNorm [39]	125.59	72.87	79.71	235.50	73.23	83.35	356.88	55.80	87.80	70.34
	OpenMix [49]	85.66	63.82	85.25	342.16	87.03	69.27	406.80	70.37	80.25	73.68
	TAL	98.40	66.57	83.55	260.84	78.84	80.07	353.66	55.90	87.08	72.45
	FMFP [48]	69.83	62.17	87.15	284.13	81.77	74.98	345.37	62.99	84.86	75.18
	TAL w/ FMFP	74.74	67.99	84.82	224.72	64.66	86.00	310.57	46.33	90.48	75.59
WRNet [45]	MSP [14]	57.60	60.13	87.47	264.67	80.04	79.41	321.39	57.26	87.23	78.55
	Cosine [47]	56.68	58.65	87.56	279.53	81.60	77.91	334.04	57.96	86.08	78.55
	Energy [23]	66.33	65.64	84.73	257.78	78.93	80.83	323.27	58.70	87.07	78.55
	MaxLogit[14]	64.85	62.70	85.36	258.57	79.35	80.67	322.42	56.89	87.29	78.55
	Entropy [33]	59.31	62.78	86.80	260.92	79.50	80.26	320.66	56.92	87.40	78.55
	Mahalanobis [4]	76.43	72.99	81.44	231.16	61.11	85.74	312.53	50.49	88.73	78.55
	Gradnorm [16]	134.85	76.20	68.51	305.28	75.61	75.57	405.68	65.57	77.46	78.55
	SIRC [40]	59.57	63.38	86.70	259.93	77.99	80.50	320.35	56.93	87.45	78.55
	LogitNorm [39]	78.86	65.56	82.68	204.45	58.98	89.10	294.87	41.88	92.03	77.15
	OpenMix [49]	50.05	56.36	88.73	251.49	74.33	81.16	304.35	51.75	88.59	79.52
	TAL	60.54	60.46	86.79	236.98	80.00	82.88	301.32	53.54	89.74	78.14
	FMFP [48]	41.60	56.65	89.50	245.10	75.71	81.42	290.23	55.63	88.89	81.07
	TAL w/ FMFP	46.71	61.16	87.49	209.80	61.18	88.32	270.90	40.63	92.50	80.98
DenseNet [15]	MSP[14]	79.06	63.62	85.75	257.69	77.86	79.77	333.86	57.58	87.64	74.62
	Cosine [47]	82.36	63.65	84.72	250.14	77.01	81.48	332.18	53.82	88.28	74.62
	Energy [23]	108.80	72.79	78.73	240.11	75.65	82.81	341.87	58.95	86.94	74.62
	MaxLogit[14]	105.98	70.20	79.60	240.06	75.65	82.86	339.68	56.69	87.39	74.62
	Entropy [33]	79.94	65.41	85.46	250.68	75.54	81.34	330.88	53.97	88.30	74.62
	Mahalanobis [4]	159.95	95.30	64.54	208.53	54.83	89.23	358.90	63.29	84.93	74.62
	Gradnorm [16]	249.85	94.73	49.88	310.37	80.45	73.68	483.52	83.21	68.79	74.62
	SIRC [40]	80.21	65.41	85.37	249.73	74.48	81.58	330.63	53.32	88.36	74.62
	LogitNorm [39]	109.80	73.28	78.90	216.63	60.21	87.27	330.07	48.43	89.50	73.80
	OpenMix [49]	64.11	59.52	87.29	267.67	79.70	78.27	328.27	58.83	86.79	77.03
	TAL	81.73	63.87	84.39	219.48	67.16	86.43	309.96	45.16	91.12	75.14
	FMFP [48]	56.67	62.45	87.72	258.04	77.11	79.31	314.57	59.81	87.37	77.96
	TAL w/ FMFP	63.36	67.65	85.42	201.70	51.51	90.23	284.61	37.53	92.94	77.85

4.2 Comparisions with the Baseline on ImageNet.

Table 2: Evaluation results of the proposed TAL on ImageNet.

Architecture	Method	Old setting FD			OOD Detection			New setting FD			ID-ACC
		AURC↓	FPR95↓	AUROC↑	AURC↓	FPR95↓	AUROC↑	AURC↓	FPR95↓	AUROC↑	
						Imagenet vs. Textures					
ResNet50	MSP [14]	72.73	63.95	86.18	301.27	46.01	87.21	351.26	49.64	86.99	76.13
	Cosine [47]	102.98	69.93	79.49	298.35	50.64	87.54	359.74	54.43	86.17	76.13
	Energy [23]	118.66	76.33	75.81	279.16	35.64	90.47	351.93	43.69	87.74	76.13
	MaxLogit [14]	113.35	72.11	77.29	278.52	34.1	90.57	349.3	41.59	88.1	76.13
	Entropy [33]	74.61	67.07	85.48	292.54	38.3	88.92	344.73	43.95	88.27	76.13
	Mahalanobis [4]	208.22	96.19	54.23	288.17	57.61	86.51	397.18	65.34	80.22	76.13
	Residual [40]	238.18	97.01	49.0	316.1	57.77	83.89	431.12	65.55	77.12	76.13
	Gradnorm [16]	206.99	89.66	57.88	272.83	30.21	91.55	385.97	42.45	84.89	76.13
	SIRC [40]	72.91	63.67	86.11	295.13	38.88	88.53	346.42	43.82	88.03	76.13
	TAL	64.66	64.93	87.11	290.5	47.66	87.51	338.45	50.11	88.29	76.43
	TAL+SIRC	64.55	63.66	87.15	288.23	46.91	87.88	336.56	49.68	88.35	76.43
						Imagenet vs. WILDS					
ResNet50	MSP [14]	72.73	63.95	86.18	272.93	59.27	87.72	326.85	60.19	87.42	76.13
	Cosine [47]	102.98	69.93	79.49	255.91	68.67	89.85	326.97	68.92	87.81	76.13
	Energy [23]	118.66	76.33	75.81	235.88	37.67	94.22	318.89	45.27	90.60	76.13
	MaxLogit [14]	113.35	72.11	77.29	237.28	38.93	93.97	317.46	45.46	90.69	76.13
	Entropy [33]	74.61	67.07	85.48	259.01	51.20	90.44	316.26	54.32	89.47	76.13
	Mahalanobis [4]	208.22	96.19	54.23	264.11	77.17	88.20	382.46	80.91	81.51	76.13
	Residual [40]	238.18	97.01	49.00	282.46	81.30	85.09	409.89	84.39	77.99	76.13
	Gradnorm [16]	206.99	89.66	57.88	237.31	25.37	94.84	363.03	38.02	87.56	76.13
	SIRC [40]	72.91	63.67	86.11	267.33	52.17	89.03	322.41	54.43	88.46	76.13
	TAL (ours)	64.66	64.93	87.11	232.11	40.97	94.28	288.67	45.55	92.91	76.43

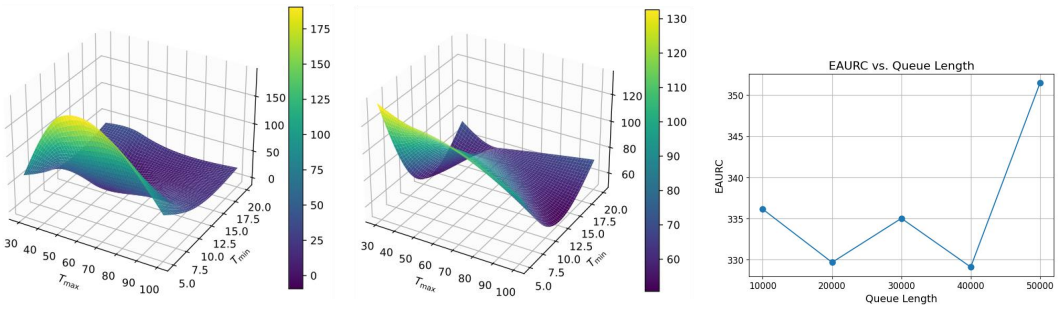

(a) EAURC vs. T_{max} , T_{min} on CIFAR10 (b) EAURC vs. T_{max} , T_{min} on CIFAR100 (c) EAURC vs. Quene Length

Figure 4: (a) and (b) is the ablation study of T_{min}, T_{max}. And (c) is the ablation study on the length of the Historical Feature Queue.

To showcase the scalability of our approach, we present the results on ImageNet in Table 2. It is obvious that our TAL strategy consistently enhances the failure detection performance of the baseline method, significantly improving the reliability of confidence. Notably, TAL reduces the AURC by 3.7 and 11.6 points, indicating a better overall performance in distinguishing between correct and incorrect predictions. It is worth noting that TAL achieves these impressive improvements while maintaining a comparable accuracy to the MSP baseline.

Additionally, we present the Risk-Coverage (RC) curves (Fig. 5(c)) for both old and new FD task settings on ImageNet. The comparison between TAL and baseline RC curves demonstrates the effectiveness of our method. Fig. 5(d) further visualizes typical and atypical data examples. For the fish category in ImageNet, typical data includes common fish images, while atypical data comprises both rare fish images from ImageNet and out-of-distribution samples.

4.3 Ablation Study

The ablation study of key components. We conduct experimental ablations on the components of our TAL loss with CIFAR100. The results are summarized in Table 3. With the dynamic magnitude $T(\tau)$ strategy, we achieve substantial enhancements in Failure Detection performance, which manifests the effectiveness of integrating typicalness-aware strategies into training approaches.

Table 3: Ablation of the key components. **Best** are bolded and <u>second best</u> are underlined. AURC and EAURC are multiplied by 10^3, the remaining metrics are percentages except ACC. "Fixed T" means the dynamic magnitude $T(\tau)$ in TAL is not adopted.

Method	Setting	AURC ↓	EAURC ↓	AUROC ↑	FPR95 ↓	TNR95 ↑	AUPR-Success ↑	AUPR-Error ↑	ACC ↑
Fixed T	Old FD	108.46	58.81	83.87	62.76	37.24	92.23	68.35	0.70
	New FD	355.62	**69.67**	88.74	53.45	46.52	**83.78**	92.51	0.70
Fixed T + Cross entropy	Old FD	99.60	55.63	83.57	65.65	34.35	92.81	66.00	0.72
	New FD	362.77	85.41	86.66	57.00	43.00	80.57	91.10	0.72
TAL loss (Dynamic T) + Cross entropy	Old FD	**94.33**	**49.43**	**85.58**	**61.24**	**38.69**	**93.56**	**68.70**	**0.72**
	New FD	**351.49**	<u>72.69</u>	**88.92**	**47.44**	**52.46**	<u>83.03</u>	**92.86**	**0.72**

The impacts of T_{min} and T_{max}. We perform an ablation study using ResNet110 on the CIFAR10 and CIFAR100 datasets to examine the impact of T_{min} and T_{max} on failure detection performance. Fig. 4 (a) and Fig. 4 (b) present the experimental results of the failure detection metric EAURC for CIFAR10 and CIFAR100, respectively. Darker regions in the figures correspond to lower values of the metric, indicating superior failure detection performance. The findings suggest that while T_{min} should not be set too small, a moderate increase in T_{max} can enhance failure detection capabilities.

The effects of the length of Historical Feature Queue. We conduct an ablation study on the CIFAR100 dataset to examine the impact of queue length on failure detection performance. The original CIFAR100 dataset consists of 50,000 training images, with 5,000 images reserved for validation and the remaining 45,000 images used for training. The results, depicted in Figure 4 (c), demonstrate that queue lengths ranging from 10,000 to 50,000 yield similar failure detection performance. However, when the queue length exceeds 50,000, there is a noticeable decline in failure detection performance.

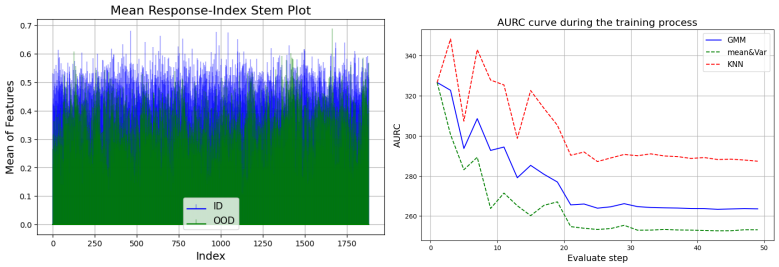

(a) Mean of features (b) Typicalness measurement

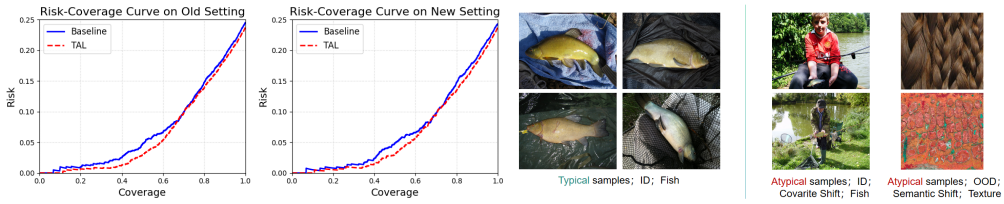

(c) RC curves (d) Typical and atypical examples

Figure 5: (a) Comparison of the Mean of Features between ID and OOD; (b) Comparison of different methods for measuring typicality; (c) The Risk-Coverage curves on old and new setting FD tasks; (d) Examples of typical and atypical examples.

Ablation of Typicality Measures. As depicted in Fig. 5 (b), we have conduced extra ablation experiments with K-nearest neighbor (KNN) distance and Gaussian Mixture Models (GMM) to assess typicality. These alternative measures did not enhance performance (lower AURC is preferable), thereby reinforcing the validity of our selection of mean/variance criteria.

5 Concluding Remarks

Summary. This paper introduces Typicalness-Aware Learning (TAL), a novel approach for mitigating overconfidence in DNNs and improving failure detection performance. The effectiveness of TAL can be attributed to a crucial insight: overconfidence in deep neural networks (DNNs) may arise when models are compelled to conform to labels that inadequately describe the image content of atypical samples. To address this issue, TAL leverages the concept of typicalness to differentiate the optimization of typical and atypical samples, thereby enhancing the reliability of confidence scores. Extensive experiments have been conducted to validate the effectiveness and robustness of TAL. We hope TAL can inspire new ideas for further enhancing the trustworthiness of deep learning models.

Limitations. The main contribution of TAL lies in recognizing the issue of overfitting atypical samples as a cause of overconfidence and proposing a comprehensive framework to tackle this problem. Given that the methods adopted in this work are simple yet effective, there is still potential for further improvement by incorporating more advanced designs, such as the methods for typicalness calculation and the dynamic magnitude generation. These are left as future work to be explored.

Broader impacts. As deep learning models become increasingly integrated into critical systems, from autonomous vehicles to medical diagnostics, the need for accurate and reliable confidence scores is paramount. TAL's ability to improve failure detection performance directly addresses this need, potentially leading to safer and more dependable AI systems.

Acknowledgments

This work was supported by National Natural Science Foundation of China (grant No. 62376068, grant No. 62350710797), by Guangdong Basic and Applied Basic Research Foundation (grant No. 2023B1515120065), by Shenzhen Science and Technology Innovation Program (grant No. JCYJ20220818102414031).

References

[1] Kendrick Boyd, Kevin H Eng, and C David Page. Area under the precision-recall curve: point estimates and confidence intervals. In *Proceedings of the European Conference on Machine Learning and Principles and Practice of Knowledge Discovery in Databases (ECML-PKDD)*, pages 451–466. Springer, 2013.

[2] Andrew P Bradley. The use of the area under the roc curve in the evaluation of machine learning algorithms. *Pattern Recognition (PR)*, 30(7):1145–1159, 1997.

[3] Mircea Cimpoi, Subhransu Maji, Iasonas Kokkinos, Sammy Mohamed, and Andrea Vedaldi. Describing textures in the wild. In *Proceedings of the IEEE conference on computer vision and pattern recognition*, pages 3606–3613, 2014.

[4] Roy De Maesschalck, Delphine Jouan-Rimbaud, and Désiré L Massart. The mahalanobis distance. *Chemometrics and intelligent laboratory systems*, 50(1):1–18, 2000.

[5] Jia Deng, Wei Dong, Richard Socher, Li-Jia Li, Kai Li, and Li Fei-Fei. Imagenet: A large-scale hierarchical image database. In *Proceedings of the IEEE/CVF Conference on Computer Vision and Pattern Recognition (CVPR)*, pages 248–255. Ieee, 2009.

[6] Alexey Dosovitskiy, Lucas Beyer, Alexander Kolesnikov, Dirk Weissenborn, Xiaohua Zhai, Thomas Unterthiner, Mostafa Dehghani, Matthias Minderer, Georg Heigold, Sylvain Gelly, et al. An image is worth 16x16 words: Transformers for image recognition at scale. *arXiv preprint arXiv:2010.11929*, 2020.

[7] Ran El-Yaniv et al. On the foundations of noise-free selective classification. *Journal of Machine Learning Research (JMLR)*, 11(5), 2010.

[8] Andre Esteva, Brett Kuprel, Roberto A Novoa, Justin Ko, Susan M Swetter, Helen M Blau, and Sebastian Thrun. Dermatologist-level classification of skin cancer with deep neural networks. *Nature*, 542(7639):115–118, 2017.

[9] Ido Galil, Mohammed Dabbah, and Ran El-Yaniv. What can we learn from the selective prediction and uncertainty estimation performance of 523 imagenet classifiers? In *Proceedings of the International Conference on Learning Representations (ICLR)*, 2023.

[10] Yonatan Geifman, Guy Uziel, and Ran El-Yaniv. Bias-reduced uncertainty estimation for deep neural classifiers. *arXiv preprint arXiv:1805.08206*, 2018.

[11] Ian J Goodfellow, Yaroslav Bulatov, Julian Ibarz, Sacha Arnoud, and Vinay Shet. Multi-digit number recognition from street view imagery using deep convolutional neural networks. *arXiv preprint arXiv:1312.6082*, 2013.

[12] Kaiming He, Xiangyu Zhang, Shaoqing Ren, and Jian Sun. Deep residual learning for image recognition. In *Proceedings of the IEEE/CVF Conference on Computer Vision and Pattern Recognition (CVPR)*, June 2016.

[13] Kaiming He, Xiangyu Zhang, Shaoqing Ren, and Jian Sun. Identity Mappings in Deep Residual Networks. In *Proceedings of the Europeon Conference on Computer Vision (ECCV)*, volume 9908, pages 630–645. Springer International Publishing, Cham, 2016. Series Title: Lecture Notes in Computer Science.

[14] Dan Hendrycks and Kevin Gimpel. A baseline for detecting misclassified and out-of-distribution examples in neural networks. *arXiv preprint arXiv:1610.02136*, 2016.

[15] Gao Huang, Zhuang Liu, Laurens Van Der Maaten, and Kilian Q. Weinberger. Densely Connected Convolutional Networks. In *Proceedings of the IEEE/CVF Conference on Computer Vision and Pattern Recognition (CVPR)*, pages 2261–2269, Honolulu, HI, July 2017. IEEE.

[16] Rui Huang, Andrew Geng, and Yixuan Li. On the importance of gradients for detecting distributional shifts in the wild. *Advances in Neural Information Processing Systems*, 34:677–689, 2021.

[17] Paul F Jaeger, Carsten Tim Lüth, Lukas Klein, and Till J. Bungert. A call to reflect on evaluation practices for failure detection in image classification. In *Proceedings of the International Conference on Learning Representations (ICLR)*, 2023.

[18] Joel Janai, Fatma Güney, Aseem Behl, Andreas Geiger, et al. Computer vision for autonomous vehicles: Problems, datasets and state of the art. *Foundations and Trends® in Computer Graphics and Vision (FOUND TRENDS COMPUT)*, 12(1–3):1–308, 2020.

[19] Pang Wei Koh, Shiori Sagawa, Henrik Marklund, Sang Michael Xie, Marvin Zhang, Akshay Balsubramani, Weihua Hu, Michihiro Yasunaga, Richard Lanas Phillips, Irena Gao, et al. Wilds: A benchmark of in-the-wild distribution shifts. In *International conference on machine learning*, pages 5637–5664. PMLR, 2021.

[20] A. Krizhevsky and G. Hinton. Learning multiple layers of features from tiny images. *Master's thesis, Department of Computer Science, University of Toronto*, 2009.

[21] Xin Lai, Zhuotao Tian, Yukang Chen, Yanwei Li, Yuhui Yuan, Shu Liu, and Jiaya Jia. Lisa: Reasoning segmentation via large language model. *arXiv preprint arXiv:2308.00692*, 2023.

[22] Tsung-Yi Lin, Priya Goyal, Ross Girshick, Kaiming He, and Piotr Dollár. Focal loss for dense object detection. In *Proceedings of the IEEE International Conference on Computer Vision (ICCV)*, pages 2980–2988, 2017.

[23] Weitang Liu, Xiaoyun Wang, John Owens, and Yixuan Li. Energy-based Out-of-distribution Detection. In *Proceedings of the Advances in Neural Information Processing Systems (NeurIPS)*, volume 33, pages 21464–21475. Curran Associates, Inc., 2020.

[24] Xiaoliu Luo, Zhuotao Tian, Taiping Zhang, Bei Yu, Yuan Yan Tang, and Jiaya Jia. Pfenet++: Boosting few-shot semantic segmentation with the noise-filtered context-aware prior mask. *IEEE Transactions on Pattern Analysis and Machine Intelligence*, 46(2):1273–1289, 2024.

[25] Jooyoung Moon, Jihyo Kim, Younghak Shin, and Sangheum Hwang. Confidence-Aware Learning for Deep Neural Networks. In *Proceedings of the International Conference on Machine Learning (ICML)*, pages 7034–7044. PMLR, November 2020. ISSN: 2640-3498.

[26] Rafael Müller, Simon Kornblith, and Geoffrey E Hinton. When does label smoothing help? *Proceedings of the Advances in Neural Information Processing Systems (NeurIPS)*, 32, 2019.

[27] Mahdi Pakdaman Naeini, Gregory Cooper, and Milos Hauskrecht. Obtaining well calibrated probabilities using bayesian binning. In *Proceedings of the AAAI conference on artificial intelligence (AAAI)*, volume 29, 2015.

[28] Bohao Peng, Zhuotao Tian, Xiaoyang Wu, Chenyao Wang, Shu Liu, Jingyong Su, and Jiaya Jia. Hierarchical dense correlation distillation for few-shot segmentation. In *Proceedings of the IEEE/CVF Conference on Computer Vision and Pattern Recognition (CVPR)*, 2023.

[29] Bohao Peng, Xiaoyang Wu, Li Jiang, Yukang Chen, Hengshuang Zhao, Zhuotao Tian, and Jiaya Jia. Oa-cnns: Omni-adaptive sparse cnns for 3d semantic segmentation. In *CVPR*, 2024.

[30] Keke Tang, Chao Hou, Weilong Peng, Runnan Chen, Peican Zhu, Wenping Wang, and Zhihong Tian. Cores: Convolutional response-based score for out-of-distribution detection. In *Proceedings of the IEEE/CVF Conference on Computer Vision and Pattern Recognition*, pages 10916–10925, 2024.

[31] Longxiang Tang, Zhuotao Tian, Kai Li, Chunming He, Hantao Zhou, Hengshuang Zhao, Xiu Li, and Jiaya Jia. Mind the interference: Retaining pre-trained knowledge in parameter efficient continual learning of vision-language models. *arXiv preprint arXiv:2407.05342*, 2024.

[32] Sunil Thulasidasan, Gopinath Chennupati, Jeff A Bilmes, Tanmoy Bhattacharya, and Sarah Michalak. On mixup training: Improved calibration and predictive uncertainty for deep neural networks. *Proceedings of the Advances in Neural Information Processing Systems (NeurIPS)*, 32, 2019.

[33] Yu Tian, Yuyuan Liu, Guansong Pang, Fengbei Liu, Yuanhong Chen, and Gustavo Carneiro. Pixel-wise energy-biased abstention learning for anomaly segmentation on complex urban driving scenes. In *Proceedings of the Europeon Conference on Computer Vision (ECCV)*, pages 246–263. Springer, 2022.

[34] Zhuotao Tian, Jiequan Cui, Li Jiang, Xiaojuan Qi, Xin Lai, Yixin Chen, Shu Liu, and Jiaya Jia. Learning context-aware classifier for semantic segmentation. In *Proceedings of the Thirty-Seventh AAAI Conference on Artificial Intelligence*, 2023.

[35] Zhuotao Tian, Xin Lai, Li Jiang, Shu Liu, Michelle Shu, Hengshuang Zhao, and Jiaya Jia. Generalized few-shot semantic segmentation. In *Proceedings of the IEEE/CVF Conference on Computer Vision and Pattern Recognition (CVPR)*, 2022.

[36] Zhuotao Tian, Michelle Shu, Pengyuan Lyu, Ruiyu Li, Chao Zhou, Xiaoyong Shen, and Jiaya Jia. Learning shape-aware embedding for scene text detection. In *Proceedings of the IEEE/CVF Conference on Computer Vision and Pattern Recognition (CVPR)*, June 2019.

[37] Zhuotao Tian, Hengshuang Zhao, Michelle Shu, Zhicheng Yang, Ruiyu Li, and Jiaya Jia. Prior guided feature enrichment network for few-shot segmentation. *TPAMI*, 2020.

[38] Hugo Touvron, Matthieu Cord, Matthijs Douze, Francisco Massa, Alexandre Sablayrolles, and Hervé Jégou. Training data-efficient image transformers & distillation through attention, January 2021. arXiv:2012.12877 [cs].

[39] Hongxin Wei, Renchunzi Xie, Hao Cheng, Lei Feng, Bo An, and Yixuan Li. Mitigating Neural Network Overconfidence with Logit Normalization. In *Proceedings of the International Conference on Machine Learning (ICML)*, pages 23631–23644. PMLR, June 2022. ISSN: 2640-3498.

[40] Guoxuan Xia and Christos-Savvas Bouganis. Augmenting softmax information for selective classification with out-of-distribution data. In *Proceedings of the Asian Conference on Computer Vision*, pages 1995–2012, 2022.

[41] Senqiao Yang, Jiaming Liu, Ray Zhang, Mingjie Pan, Zoey Guo, Xiaoqi Li, Zehui Chen, Peng Gao, Yandong Guo, and Shanghang Zhang. Lidar-llm: Exploring the potential of large language models for 3d lidar understanding. *arXiv preprint arXiv:2312.14074*, 2023.

[42] Senqiao Yang, Zhuotao Tian, Li Jiang, and Jiaya Jia. Unified language-driven zero-shot domain adaptation. In *Proceedings of the IEEE/CVF Conference on Computer Vision and Pattern Recognition*, pages 23407–23415, 2024.

[43] Mert Yuksekgonul, Linjun Zhang, James Y Zou, and Carlos Guestrin. Beyond confidence: Reliable models should also consider atypicality. *Advances in Neural Information Processing Systems*, 36, 2024.

[44] Sukmin Yun, Jongjin Park, Kimin Lee, and Jinwoo Shin. Regularizing class-wise predictions via self-knowledge distillation. In *Proceedings of the IEEE/CVF Conference on Computer Vision and Pattern Recognition (CVPR)*, pages 13876–13885, 2020.

[45] Sergey Zagoruyko and Nikos Komodakis. Wide Residual Networks. In *Proceedings of the British Machine Vision Conference (BMVC)*, York, France, January 2016. British Machine Vision Association. arXiv:1605.07146 [cs].

[46] Xu-Yao Zhang, Cheng-Lin Liu, and Ching Y Suen. Towards robust pattern recognition: A review. *Proceedings of the IEEE (P-IEEE)*, 108(6):894–922, 2020.

[47] Zihan Zhang and Xiang Xiang. Decoupling maxlogit for out-of-distribution detection. In *Proceedings of the IEEE/CVF Conference on Computer Vision and Pattern Recognition (CVPR)*, pages 3388–3397, 2023.

[48] Fei Zhu, Zhen Cheng, Xu-Yao Zhang, and Cheng-Lin Liu. Rethinking confidence calibration for failure prediction. In *Proceedings of the Europeon Conference on Computer Vision (ECCV)*, pages 518–536. Springer, 2022.

[49] Fei Zhu, Zhen Cheng, Xu-Yao Zhang, and Cheng-Lin Liu. Openmix: Exploring outlier samples for misclassification detection. In *Proceedings of the IEEE/CVF Conference on Computer Vision and Pattern Recognition (CVPR)*, pages 12074–12083, 2023.

[50] Jianing Zhu, Hengzhuang Li, Jiangchao Yao, Tongliang Liu, Jianliang Xu, and Bo Han. Unleashing mask: Explore the intrinsic out-of-distribution detection capability. In *Proceedings of the International Conference on Machine Learning (ICML)*, pages 43068–43104. PMLR, 2023.

Appendix

Overview

This is the supplementary material for our submission titled *Typicalness-Aware Learning for Failure Detection*. This material supplements the main paper with the following content:

- A. **More Experimental Details**
  - A.1. Baselines
  - A.2. Evaluation Metrics
  - A.3. Training Configuration
  - A.4. Test Configuration
- B. **The Reasons Why OoD method Performs Poor in FD**
- C. **Additional Results**

A More Experimental Details

A.1 Baselines

We compare our proposed TAL method against eleven baseline approaches for failure detection. ① Maximum Softmax Probability (MSP), ② MaxLogit[14] and ③ Cosine[47] utilize the maximum softmax probability of $\boldsymbol{f}$, the maximum logit ($\boldsymbol{f}$) value and the cosine similarity between the $\boldsymbol{f}$ and the corresponding label's one-hot vector as the confidence score, respectively. ④ Energy Score [23] uses the negative energy of the softmax output as the confidence score. ⑤ LogitNorm [39] normalizes the logits to a fixed magnitude to improve confidence score reliability. ⑥ Entropy [33] employs the entropy of the softmax distribution as an uncertainty measure. ⑦ Mahalanobis [4] computes confidence scores based on the Mahalanobis distance in the feature space. ⑧ Gradnorm [16] utilizes the gradient norm of the loss with respect to the model parameters as a measure of uncertainty. ⑨ OpenMix [49], a SOTA OOD detection method, leverages data augmentation techniques to enhance confidence score separation between in-distribution and out-of-distribution samples. ⑩ SIRC [40] augments softmax-based confidence scores with feature-agnostic information to better identify OOD samples while maintaining separation between correct and incorrect ID predictions. ⑪ Failure Misclassification Feature Propagation (FMFP) [48], a SOTA failure detection method, focuses on improving model accuracy and confidence score reliability through stochastic weight averaging (SWA) and sharpness-aware minimization (SAM). We also explore combining the proposed TAL with FMFP (⑫) to investigate their complementary effects.

A.2 Evaluation Metrics

To comprehensively assess the performance of TAL in failure detection, we adopt nine widely recognized evaluation metrics [17, 48, 9], including Area Under the Risk-Coverage Curve (AURC), Excess Area Under the Risk-Coverage Curve (EAURC), Area Under the Receiver Operating Characteristic Curve (AUROC), False Positive Rate at 95% True Positive Rate (FPR95), True Negative Rate at 95% True Positive Rate (TNR95), Area Under the Precision-Recall curve of Suceess and Error (AUPR_Success and AUPR_Error). ① AURC [7]: Area Under the Risk-Coverage Curve, depicting the error rate as a function of confidence thresholds. ② EAURC [10]: Excess Area Under the Risk-Coverage Curve, evaluating the ranking ability of confidence scores. ③ AUROC [2]: Area Under the Receiver Operating Characteristic Curve, illustrating the trade-off between true positive rate (TPR) and false positive rate (FPR). ④: False Positive Rate at 95% True Positive Rate. ⑤: True Negative Rate at 95% True Positive Rate. ⑦ AUPR_Success[1] and ⑧ AUPR_Success represent two approximations for estimating the Area Under the Precision-Recall curve (AUPR), with AUPR_Success sampling thresholds from positive scores while AUPR_Error utilizes only scores of observed positive and negative instances as thresholds. ⑨: Test accuracy, providing a reference for overall model performance.

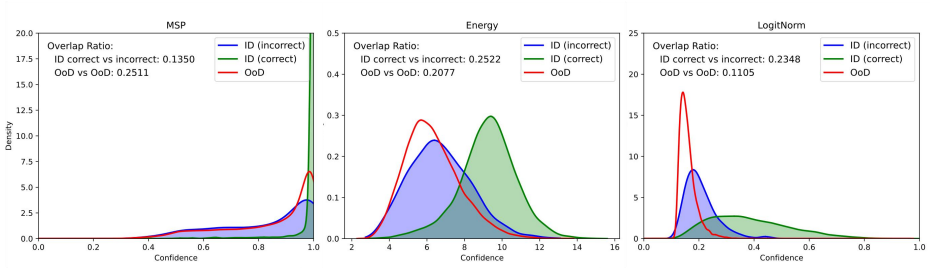

Figure 6: OOD-D methods lead to worse confidence separation between correct and wrong samples.

A.3 Training Configuration

For experiments on the CIFAR [20], we employ an SGD optimizer with an initial learning rate of 0.1, a momentum of 0.9, and a weight decay of 0.0005. The models are trained for 200 epochs with a batch size of 256 on a single NVIDIA GeForce RTX 3090 GPU. Furthermore, we adopt a CosineAnnealingLR scheduler to adjust the learning rate during training. On ImageNet [5], we use the ResNet-50 architecture as our backbone. The models are trained for 90 epochs with an initial learning rate of 0.1 on a single NVIDIA A100. The learning rate is decayed by a factor of 0.1 every 30 epochs.

A.4 Evaluation Configuration

To ensure a fair and robust evaluation, we conduct experiments with three independent training runs on CIFAR100, each using a different random seed. All baseline methods and our proposed TAL are evaluated using identical settings across these three runs. The final performance metrics reported in our results are averaged across these three sets of weights to account for training variance. For clarity of presentation, we multiply AURC values by 10^3, while maintaining all other metrics in percentage form. This systematic evaluation approach allows us to make reliable comparisons between different methods while accounting for the inherent variability in deep learning model training.

For ImageNet experiments, we encountered several implementation challenges with some baseline methods. Specifically, FMFP failed to achieve competitive accuracy, while LogitNorm and OpenMix suffered from training instability and collapse. These issues might be attributed to the fact that these methods were not originally validated on ImageNet in their respective papers. While it might be possible to adapt these methods for ImageNet through extensive parameter tuning and modifications, such adaptations would require significant engineering effort and might deviate from the original methods. Therefore, we opted not to report results for these methods on ImageNet to maintain experimental integrity.

B The Reasons Why OoD method Performs Poor in FD

It is interesting to note that in the Old Few-Shot Detection (FD) setting, most Out-of-Distribution (OoD) methods, such as Energy Score and LogitNorm, exhibit poor performance compared to baseline methods like Maximum Softmax Probability (MSP) and MaxLogit. This decline in performance can be attributed to the fact that while OoD methods effectively increase the confidence score gap between in-distribution and out-of-distribution samples, they inadvertently disrupt the natural confidence score hierarchy within the in-distribution samples. As a result, there is a greater overlap in the confidence distributions of correctly and incorrectly predicted in-distribution samples, as illustrated in Fig. 6. This observation highlights the importance of developing dedicated FD methods that can effectively distinguish between correct and incorrect predictions within the in-distribution data.

C Additional Results

Evaluation on Transformer-based architectures.

Considering the remarkable success of vision transformers as network architectures, it is crucial to incorporate a transformer-based network in our analysis and evaluate the effectiveness of our proposed

method. It is worth noting that the substantial disparities between ViT [6] and CNN architectures in terms of their design, feature representation, and learning mechanisms may pose challenges in directly applying methods that have proven effective on CNNs to ViT models.

Implementation Details of ViT. TAL can also be applied to Transformer architectures. However, it is important to note that certain CNN-based methods may not perform well on Transformer-based tasks. For example, the accuracy of OpenMix with default settings is significantly lower (approximately 0.20) compared to the baseline. This indicates that OpenMix, originally designed for CNNs, does not effectively detect failures when applied to ViT models without appropriate modifications and adjustments that consider the unique architectural characteristics of ViT.

Specifically, ViT learns the relationships between image patches through the Self-Attention mechanism, resulting in distinct feature representations and gradient flow patterns compared to CNNs. Moreover, ViT typically employs different normalization techniques, such as Layer Normalization, instead of the commonly used Batch Normalization in CNNs. These differences can impact the effectiveness of certain methods when applied to ViT. To successfully adapt these methods to ViT, appropriate modifications and adjustments may be necessary to account for the unique architectural characteristics of ViT.

To explore the performance of current popular failure detection methods on ViT models, we conducted experiments using the pre-trained DeiT-Small model ("deit_small_patch16_224") from the timm library. We employed the SGD optimizer with a base learning rate of 0.01, a weight decay of 0.0005, and a momentum of 0.9. The learning rate scheduler was set to CosineAnnealingLR, with the T_max parameter determined by total training epochs. The experiments were conducted on the CIFAR100 dataset, with a total of 25 training epochs and a batch size of 256.

Experimental Results on ViT. The experimental results shown in Tab. 4 and Tab. 5 validate the applicability of TAL to vision transformers. By prioritizing optimization with typical samples and concurrently relaxing the requirements for atypical samples, TAL effectively mitigates overconfidence and enhances failure detection performance.

Table 4: New FD Setting evaluation on CIFAR100 with ViT. Mean and standard deviations of Failure Detection performance on CIFAR benchmarks. The experimental results are reported over five epochs. **Best** are bolded and second best are underlined. AURC and EAURC are multiplied by 10^3, the remaining metrics are percentages except ACC.

Method	AURC ↓	EAURC ↓	AUROC ↑	FPR95 ↓	TNR95 ↑	AUPR-Success ↑	AUPR-Error ↑	ACC ↑
MSP [14]	269.42±5.71	60.10±5.80	89.75±1.10	49.65±4.15	50.35±4.15	88.02±1.06	91.48±1.05	0.86±0.00
LogitNorm [39]	268.20±9.40	57.84±9.90	91.25±0.99	37.78±2.18	62.19±2.17	88.03±2.05	93.38±0.61	0.86±0.00
TAL	**262.57±7.60**	**53.34±7.82**	**91.61±0.65**	**35.64±1.07**	**64.34±1.05**	**89.01±1.68**	**93.57±0.28**	**0.87±0.00**
FMFP [48]	255.89±2.99	50.37±3.56	91.09±0.69	45.11±3.19	54.86±3.21	90.02±0.63	92.40±0.73	0.87±0.00
TAL w/ FMFP	**246.07±2.21**	**39.96±2.89**	**93.17±0.76**	**31.84±2.53**	**68.15±2.46**	**91.84±0.60**	**94.41±0.68**	0.87±0.00

Table 5: Old Setting evaluation on CIFAR100 with ViT. Mean and standard deviations of Failure Detection performance on CIFAR benchmarks. The experimental results are reported over five epochs. **Best** are bolded and second best are underlined. AURC and EAURC are multiplied by 10^3, the remaining metrics are percentages except ACC.

Method	Setting	AURC ↓	EAURC ↓	AUROC ↑	FPR95 ↓	TNR95 ↑	AUPR-Success ↑	AUPR-Error ↑	ACC ↑
MSP [14]	Old FD	27.72±0.61	18.17±0.61	88.88±0.33	56.71±2.18	43.26±2.17	97.96±0.07	54.36±1.43	0.86±0.00
LogitNorm [39]	Old FD	27.46±0.32	**17.54±0.19**	89.16±0.26	56.99±1.32	42.98±1.35	**98.03±0.02**	**54.92±0.93**	0.86±0.00
TAL	Old FD	**27.15±0.33**	17.62±0.20	**89.83±0.15**	**55.65±1.62**	**44.28±1.69**	**98.03±0.02**	54.47±0.30	**0.87±0.00**
FMFP [48]	Old FD	22.58±0.31	**14.30±0.48**	**90.11±0.41**	54.35±3.27	45.62±3.27	**98.41±0.05**	54.67±2.80	0.87±0.00
TAL w/ FMFP	Old FD	**21.02±0.32**	14.55±0.21	88.79±0.54	**53.00±2.43**	**46.99±2.35**	98.15±0.07	**54.88±1.90**	0.87±0.00

NeurIPS Paper Checklist

1. **Claims**

   Question: Do the main claims made in the abstract and introduction accurately reflect the paper's contributions and scope?

   Answer: [Yes]

   Justification: The abstract and introduction clearly state the main contributions and scope of the paper, which are consistent with the theoretical and experimental results presented in the body of the paper.

   Guidelines:

   - The answer NA means that the abstract and introduction do not include the claims made in the paper.
   - The abstract and/or introduction should clearly state the claims made, including the contributions made in the paper and important assumptions and limitations. A No or NA answer to this question will not be perceived well by the reviewers.
   - The claims made should match theoretical and experimental results, and reflect how much the results can be expected to generalize to other settings.
   - It is fine to include aspirational goals as motivation as long as it is clear that these goals are not attained by the paper.

2. **Limitations**

   Question: Does the paper discuss the limitations of the work performed by the authors?

   Answer: [Yes]

   Justification: The limitations of the proposed method are discussed in the "Limitations" section.

   Guidelines:

   - The answer NA means that the paper has no limitation while the answer No means that the paper has limitations, but those are not discussed in the paper.
   - The authors are encouraged to create a separate "Limitations" section in their paper.
   - The paper should point out any strong assumptions and how robust the results are to violations of these assumptions (e.g., independence assumptions, noiseless settings, model well-specification, asymptotic approximations only holding locally). The authors should reflect on how these assumptions might be violated in practice and what the implications would be.
   - The authors should reflect on the scope of the claims made, e.g., if the approach was only tested on a few datasets or with a few runs. In general, empirical results often depend on implicit assumptions, which should be articulated.
   - The authors should reflect on the factors that influence the performance of the approach. For example, a facial recognition algorithm may perform poorly when image resolution is low or images are taken in low lighting. Or a speech-to-text system might not be used reliably to provide closed captions for online lectures because it fails to handle technical jargon.
   - The authors should discuss the computational efficiency of the proposed algorithms and how they scale with dataset size.
   - If applicable, the authors should discuss possible limitations of their approach to address problems of privacy and fairness.
   - While the authors might fear that complete honesty about limitations might be used by reviewers as grounds for rejection, a worse outcome might be that reviewers discover limitations that aren't acknowledged in the paper. The authors should use their best judgment and recognize that individual actions in favor of transparency play an important role in developing norms that preserve the integrity of the community. Reviewers will be specifically instructed to not penalize honesty concerning limitations.

3. **Theory Assumptions and Proofs**

   Question: For each theoretical result, does the paper provide the full set of assumptions and a complete (and correct) proof?

Answer: [Yes]

Justification: The paper provides theoretical analysis and justification for the proposed TAL.

Guidelines:

- The answer NA means that the paper does not include theoretical results.
- All the theorems, formulas, and proofs in the paper should be numbered and cross-referenced.
- All assumptions should be clearly stated or referenced in the statement of any theorems.
- The proofs can either appear in the main paper or the supplemental material, but if they appear in the supplemental material, the authors are encouraged to provide a short proof sketch to provide intuition.
- Inversely, any informal proof provided in the core of the paper should be complemented by formal proofs provided in appendix or supplemental material.
- Theorems and Lemmas that the proof relies upon should be properly referenced.

4. **Experimental Result Reproducibility**

   Question: Does the paper fully disclose all the information needed to reproduce the main experimental results of the paper to the extent that it affects the main claims and/or conclusions of the paper (regardless of whether the code and data are provided or not)?

   Answer: [Yes]

   Justification: The paper provides sufficient details on the experimental setup, datasets, and network architectures to reproduce the main results.

   Guidelines:

   - The answer NA means that the paper does not include experiments.
   - If the paper includes experiments, a No answer to this question will not be perceived well by the reviewers: Making the paper reproducible is important, regardless of whether the code and data are provided or not.
   - If the contribution is a dataset and/or model, the authors should describe the steps taken to make their results reproducible or verifiable.
   - Depending on the contribution, reproducibility can be accomplished in various ways. For example, if the contribution is a novel architecture, describing the architecture fully might suffice, or if the contribution is a specific model and empirical evaluation, it may be necessary to either make it possible for others to replicate the model with the same dataset, or provide access to the model. In general. releasing code and data is often one good way to accomplish this, but reproducibility can also be provided via detailed instructions for how to replicate the results, access to a hosted model (e.g., in the case of a large language model), releasing of a model checkpoint, or other means that are appropriate to the research performed.
   - While NeurIPS does not require releasing code, the conference does require all submissions to provide some reasonable avenue for reproducibility, which may depend on the nature of the contribution. For example
     (a) If the contribution is primarily a new algorithm, the paper should make it clear how to reproduce that algorithm.
     (b) If the contribution is primarily a new model architecture, the paper should describe the architecture clearly and fully.
     (c) If the contribution is a new model (e.g., a large language model), then there should either be a way to access this model for reproducing the results or a way to reproduce the model (e.g., with an open-source dataset or instructions for how to construct the dataset).
     (d) We recognize that reproducibility may be tricky in some cases, in which case authors are welcome to describe the particular way they provide for reproducibility. In the case of closed-source models, it may be that access to the model is limited in some way (e.g., to registered users), but it should be possible for other researchers to have some path to reproducing or verifying the results.

5. **Open access to data and code**

Question: Does the paper provide open access to the data and code, with sufficient instructions to faithfully reproduce the main experimental results, as described in supplemental material?

Answer: [Yes]

Justification: The code and data will be made available upon publication.

Guidelines:

- The answer NA means that paper does not include experiments requiring code.
- Please see the NeurIPS code and data submission guidelines (`https://nips.cc/public/guides/CodeSubmissionPolicy`) for more details.
- While we encourage the release of code and data, we understand that this might not be possible, so "No" is an acceptable answer. Papers cannot be rejected simply for not including code, unless this is central to the contribution (e.g., for a new open-source benchmark).
- The instructions should contain the exact command and environment needed to run to reproduce the results. See the NeurIPS code and data submission guidelines (`https://nips.cc/public/guides/CodeSubmissionPolicy`) for more details.
- The authors should provide instructions on data access and preparation, including how to access the raw data, preprocessed data, intermediate data, and generated data, etc.
- The authors should provide scripts to reproduce all experimental results for the new proposed method and baselines. If only a subset of experiments are reproducible, they should state which ones are omitted from the script and why.
- At submission time, to preserve anonymity, the authors should release anonymized versions (if applicable).
- Providing as much information as possible in supplemental material (appended to the paper) is recommended, but including URLs to data and code is permitted.

6. **Experimental Setting/Details**

Question: Does the paper specify all the training and test details (e.g., data splits, hyperparameters, how they were chosen, type of optimizer, etc.) necessary to understand the results?

Answer: [Yes]

Justification: The paper specifies the training and test details, including data splits, hyperparameters, and optimization settings.

Guidelines:

- The answer NA means that the paper does not include experiments.
- The experimental setting should be presented in the core of the paper to a level of detail that is necessary to appreciate the results and make sense of them.
- The full details can be provided either with the code, in appendix, or as supplemental material.

7. **Experiment Statistical Significance**

Question: Does the paper report error bars suitably and correctly defined or other appropriate information about the statistical significance of the experiments?

Answer: [Yes]

Justification: The paper reports mean and standard deviations of the experimental results over multiple runs.

Guidelines:

- The answer NA means that the paper does not include experiments.
- The authors should answer "Yes" if the results are accompanied by error bars, confidence intervals, or statistical significance tests, at least for the experiments that support the main claims of the paper.
- The factors of variability that the error bars are capturing should be clearly stated (for example, train/test split, initialization, random drawing of some parameter, or overall run with given experimental conditions).

- The method for calculating the error bars should be explained (closed form formula, call to a library function, bootstrap, etc.)
- The assumptions made should be given (e.g., Normally distributed errors).
- It should be clear whether the error bar is the standard deviation or the standard error of the mean.
- It is OK to report 1-sigma error bars, but one should state it. The authors should preferably report a 2-sigma error bar than state that they have a 96% CI, if the hypothesis of Normality of errors is not verified.
- For asymmetric distributions, the authors should be careful not to show in tables or figures symmetric error bars that would yield results that are out of range (e.g. negative error rates).
- If error bars are reported in tables or plots, The authors should explain in the text how they were calculated and reference the corresponding figures or tables in the text.

8. **Experiments Compute Resources**

   Question: For each experiment, does the paper provide sufficient information on the computer resources (type of compute workers, memory, time of execution) needed to reproduce the experiments?

   Answer: [Yes]

   Justification: The paper provides information on the compute resources used for the experiments in the Experiments section.

   Guidelines:

   - The answer NA means that the paper does not include experiments.
   - The paper should indicate the type of compute workers CPU or GPU, internal cluster, or cloud provider, including relevant memory and storage.
   - The paper should provide the amount of compute required for each of the individual experimental runs as well as estimate the total compute.
   - The paper should disclose whether the full research project required more compute than the experiments reported in the paper (e.g., preliminary or failed experiments that didn't make it into the paper).

9. **Code Of Ethics**

   Question: Does the research conducted in the paper conform, in every respect, with the NeurIPS Code of Ethics `https://neurips.cc/public/EthicsGuidelines`?

   Answer: [Yes]

   Justification: The research conducted in the paper conforms to the NeurIPS Code of Ethics.

   Guidelines:

   - The answer NA means that the authors have not reviewed the NeurIPS Code of Ethics.
   - If the authors answer No, they should explain the special circumstances that require a deviation from the Code of Ethics.
   - The authors should make sure to preserve anonymity (e.g., if there is a special consideration due to laws or regulations in their jurisdiction).

10. **Broader Impacts**

    Question: Does the paper discuss both potential positive societal impacts and negative societal impacts of the work performed?

    Answer: [Yes]

    Justification: In the Discussion section, the paper discusses both potential positive and negative societal impacts of the work performed.

    Guidelines:

    - The answer NA means that there is no societal impact of the work performed.
    - If the authors answer NA or No, they should explain why their work has no societal impact or why the paper does not address societal impact.

- Examples of negative societal impacts include potential malicious or unintended uses (e.g., disinformation, generating fake profiles, surveillance), fairness considerations (e.g., deployment of technologies that could make decisions that unfairly impact specific groups), privacy considerations, and security considerations.
- The conference expects that many papers will be foundational research and not tied to particular applications, let alone deployments. However, if there is a direct path to any negative applications, the authors should point it out. For example, it is legitimate to point out that an improvement in the quality of generative models could be used to generate deepfakes for disinformation. On the other hand, it is not needed to point out that a generic algorithm for optimizing neural networks could enable people to train models that generate Deepfakes faster.
- The authors should consider possible harms that could arise when the technology is being used as intended and functioning correctly, harms that could arise when the technology is being used as intended but gives incorrect results, and harms following from (intentional or unintentional) misuse of the technology.
- If there are negative societal impacts, the authors could also discuss possible mitigation strategies (e.g., gated release of models, providing defenses in addition to attacks, mechanisms for monitoring misuse, mechanisms to monitor how a system learns from feedback over time, improving the efficiency and accessibility of ML).

11. **Safeguards**

    Question: Does the paper describe safeguards that have been put in place for responsible release of data or models that have a high risk for misuse (e.g., pretrained language models, image generators, or scraped datasets)?

    Answer: [NA]

    Justification: The proposed TAL is focused on improving failure detection for general classification tasks without requiring the release of potentially unsafe data or models.

    Guidelines:

    - The answer NA means that the paper poses no such risks.
    - Released models that have a high risk for misuse or dual-use should be released with necessary safeguards to allow for controlled use of the model, for example by requiring that users adhere to usage guidelines or restrictions to access the model or implementing safety filters.
    - Datasets that have been scraped from the Internet could pose safety risks. The authors should describe how they avoided releasing unsafe images.
    - We recognize that providing effective safeguards is challenging, and many papers do not require this, but we encourage authors to take this into account and make a best faith effort.

12. **Licenses for existing assets**

    Question: Are the creators or original owners of assets (e.g., code, data, models), used in the paper, properly credited and are the license and terms of use explicitly mentioned and properly respected?

    Answer: [Yes]

    Justification: The paper properly credits and mentions the licenses for existing assets used.

    Guidelines:

    - The answer NA means that the paper does not use existing assets.
    - The authors should cite the original paper that produced the code package or dataset.
    - The authors should state which version of the asset is used and, if possible, include a URL.
    - The name of the license (e.g., CC-BY 4.0) should be included for each asset.
    - For scraped data from a particular source (e.g., website), the copyright and terms of service of that source should be provided.
    - If assets are released, the license, copyright information, and terms of use in the package should be provided. For popular datasets, `paperswithcode.com/datasets` has curated licenses for some datasets. Their licensing guide can help determine the license of a dataset.

- For existing datasets that are re-packaged, both the original license and the license of the derived asset (if it has changed) should be provided.
- If this information is not available online, the authors are encouraged to reach out to the asset's creators.

13. **New Assets**

    Question: Are new assets introduced in the paper well documented and is the documentation provided alongside the assets?

    Answer: [Yes]

    Justification: The paper introduces new codes, which will be documented in the github link.

    Guidelines:

    - The answer NA means that the paper does not release new assets.
    - Researchers should communicate the details of the dataset/code/model as part of their submissions via structured templates. This includes details about training, license, limitations, etc.
    - The paper should discuss whether and how consent was obtained from people whose asset is used.
    - At submission time, remember to anonymize your assets (if applicable). You can either create an anonymized URL or include an anonymized zip file.

14. **Crowdsourcing and Research with Human Subjects**

    Question: For crowdsourcing experiments and research with human subjects, does the paper include the full text of instructions given to participants and screenshots, if applicable, as well as details about compensation (if any)?

    Answer: [NA]

    Justification: The paper does not involve crowdsourcing or research with human subjects.

    Guidelines:

    - The answer NA means that the paper does not involve crowdsourcing nor research with human subjects.
    - Including this information in the supplemental material is fine, but if the main contribution of the paper involves human subjects, then as much detail as possible should be included in the main paper.
    - According to the NeurIPS Code of Ethics, workers involved in data collection, curation, or other labor should be paid at least the minimum wage in the country of the data collector.

15. **Institutional Review Board (IRB) Approvals or Equivalent for Research with Human Subjects**

    Question: Does the paper describe potential risks incurred by study participants, whether such risks were disclosed to the subjects, and whether Institutional Review Board (IRB) approvals (or an equivalent approval/review based on the requirements of your country or institution) were obtained?

    Answer: [NA]

    Justification: The paper does not involve research with human subjects.

    Guidelines:

    - The answer NA means that the paper does not involve crowdsourcing nor research with human subjects.
    - Depending on the country in which research is conducted, IRB approval (or equivalent) may be required for any human subjects research. If you obtained IRB approval, you should clearly state this in the paper.
    - We recognize that the procedures for this may vary significantly between institutions and locations, and we expect authors to adhere to the NeurIPS Code of Ethics and the guidelines for their institution.
    - For initial submissions, do not include any information that would break anonymity (if applicable), such as the institution conducting the review.